

circEYA1 Functions as a Sponge of miR-582-3p to Suppress Cervical Adenocarcinoma Tumorigenesis via Upregulating CXCL14

Junfen Xu,^{1,5} Yanan Zhang,^{2,5} Yongjie Huang,^{1,5} Xiaohui Dong,² Zhenzhen Xiang,³ Jian Zou,¹ Luyao Wu,¹ and Weiguo Lu^{1,4}

¹Department of Gynecologic Oncology, Women's Hospital, Zhejiang University School of Medicine, Hangzhou 310006, China; ²Zhejiang University School of Medicine, Hangzhou 310058, China; ³Women's Hospital, Zhejiang University School of Medicine, Hangzhou 310006, China; ⁴Center of Uterine Cancer Diagnosis & Therapy of Zhejiang Province, Hangzhou 310006, China

Circular RNAs (circRNAs) function as efficient microRNA (miRNA) sponges that regulate gene expression in the pathogenesis of many human malignancies. However, their roles in cervical adenocarcinoma remain largely unknown. In this study, we aimed to seek novel circRNAs that regulate cervical adenocarcinoma carcinogenesis and to explore their regulatory mechanisms as well as clinical significance. We identified that 24 circRNAs were differentially expressed in cervical adenocarcinoma tissues by RNA sequencing. Among them, circEYA1 was the most significantly downregulated circRNA in cervical adenocarcinoma. In cervical adenocarcinoma cells, circEYA1 overexpression led to suppression of cell viability and colony formation, promotion of apoptosis, and a decrease of the xenograft tumor growth. The mechanism underlying these observations is that circEYA1 functioned as a sponge of miR-582-3p and abrogated its suppression of CXCL14 expression. Consistently, miR-582-3p inhibition phenocopied the biological effects of circEYA1 overexpression in cervical adenocarcinoma cells. Moreover, miR-582-3p overexpression reversed the suppressive behaviors of circEYA1 *in vitro* and *in vivo*. In addition, the expression, correlation, and clinical diagnostic value of circEYA1/miR-582-3p/CXCL14 were confirmed in 198 clinical cervical tissue samples. In summary, our findings highlight a novel tumor suppressive role of circEYA1 in cervical adenocarcinoma tumorigenesis and may provide a potential diagnostic marker and therapeutic target for patients with cervical adenocarcinoma.

INTRODUCTION

The wide implementation of human papillomavirus (HPV) vaccines and tumor screening programs has dramatically reduced morbidity and mortality of cervical cancer in many developed countries over the past decades.¹ However, this effect is mainly attributable to a decrease in the incidence of squamous cell carcinoma. In contrast, a relative and absolute increase in the incidence of adenocarcinoma of the uterine cervix, especially among young women, has arisen over the same period.^{2–11} Changes in these rates may indicate alter-

ations in underlying screening procedures. Since the pathogenesis of cervical adenocarcinoma is not well studied, there is an urgent need to elucidate molecular mechanisms for adenocarcinoma and to identify new reliable biomarkers that allow for better diagnostic stratification and therapies.

Besides of linear RNA molecules, a newly appreciated class of non-coding RNA, circular RNAs (circRNAs) have recently caused people's attention that they are presumably stable due to their resistance to exonuclease-dependent degradations and that they can be involved in cancer development and progression.^{12–14} Studies have shown that circRNAs could act as miRNA sponges and even as protein sponges or scaffolds.^{15–17} The best-characterized role of circRNAs thus far is "miRNA sponge" in many cancers.^{18–20} For example, it was reported that circAGFG1 could act as a sponge of miR-195-5p to promote CCNE1 expression, which further result in triple-negative breast cancer (TNBC) progression.¹⁸ Zhang et al.²¹ also showed that circNRIP1 promoted gastric cancer progression by regulating the AKT1/mTOR pathway as a sponge of tumor-suppressive miR-149-5p. However, circRNAs associated with cervical adenocarcinoma have not been reported to date.

In this study, we explored the expression profile of circRNAs in cervical adenocarcinoma using RNA sequencing and identified a novel circRNA, circEYA1, derived from the EYA1 gene (circBase: hsa_circ_0137084). The screen results verified that circEYA1 was the most significantly downregulated circRNA in cervical adenocarcinoma tissues. We further found that circEYA1 could suppress cell viability and colony formation and promote cell apoptosis by acting as a sponge for miR-582-3p to relieve the repression of target gene CXCL14. In addition, investigations in a large cohort of cervical

Received 22 June 2020; accepted 19 October 2020;
<https://doi.org/10.1016/j.omtn.2020.10.026>.

⁵These authors contributed equally

Correspondence: Weiguo Lu, Department of Gynecologic Oncology, Women's Hospital, Zhejiang University School of Medicine, Hangzhou 310006, China.
E-mail: lbwg@zju.edu.cn



adenocarcinoma tissues revealed that circEYA1 was accordingly either negatively or positively correlated with miR-582-3p and CXCL14. Taken together, our studies show that circEYA1 serves as a tumor-suppressive gene in cervical adenocarcinoma, which suggests a possibility of circEYA1 as a valuable target of diagnosis and treatment for cervical adenocarcinoma.

RESULTS

circRNA Expression Profiles in Cervical Adenocarcinoma and circEYA1 Characterization

To explore which circRNAs are important in cervical adenocarcinoma, we conducted RNA sequencing (RNA-seq) analysis using 8 human cervical tissue samples (4 normal and 4 adenocarcinoma tissues). For this analysis, 2-fold change and false discovery rate (FDR) <0.05 were set as cut-off criteria. From the results, 24 circRNAs were differentially expressed in cervical adenocarcinoma comparing with normal samples, among which 10 were upregulated, while the other 14 were downregulated (Figure 1A; Table S1). This differential expression was further illustrated by the heatmap shown in Figure 1B. Among these 24 circRNAs, we aligned on 11 circRNAs with known circBase IDs (hsa_circ_0000118, hsa_circ_0000119, hsa_circ_0016599, hsa_circ_0094647, hsa_circ_0105346, hsa_circ_0058806, hsa_circ_0007054, hsa_circ_0004390, hsa_circ_6472, hsa_circ_0002538, hsa_circ_0137084). To confirm their identities, the cDNA of these circRNAs was determined by Sanger DNA sequencing. Except for hsa_circ_0016599 (data not shown), most of the results were in line with the circBase database (Figure S1). Furthermore, the expression of these 10 circRNAs was tested by qRT-PCR at the tissue levels (20 normal versus 20 adenocarcinoma tissues). We found that 7 out of 10 were consistent with the prediction by RNA-seq. Among them, 5 circRNAs (hsa_circ_0000118, hsa_circ_0094647, hsa_circ_0105346, hsa_circ_0058806, and hsa_circ_0000119) were significantly increased, whereas 2 circRNAs (hsa_circ_0137084 and hsa_circ_0004390) were significantly decreased in the cervical adenocarcinoma tissue group over the normal cervical tissue group (Figure 1C). hsa_circ_0000118 and hsa_circ_0137084 were the most up- and downregulated circRNAs, respectively. However, we experienced extremely difficult challenges to knockdown hsa_circ_0000118 by small interfering RNA (siRNAs). Thus, we only continued with hsa_circ_0137084 for further study.

To confirm the predicted downregulation of hsa_circ_0137084 in cervical adenocarcinoma tissues, we examined the expression of hsa_circ_0137084 by qRT-PCR in another panel of 20 primary cervical squamous cell carcinoma (CSCC) tissues versus 20 normal cervical tissues. The result showed that the level of hsa_circ_0137084 was not significantly decreased in CSCC (Figure S2). These data suggest that hsa_circ_0137084 is a cervical adenocarcinoma-specific circRNA. hsa_circ_0137084 arises from the EYA1 gene, which is located at chromosome 8 and consists of the head-to-tail splicing of exon 4 and exon 11 (72181974-72246409). It was designated as circEYA1 (Figure 1D). We designed the specific divergent primers to characterize circEYA1 and used convergent primers to control linear forms. The combination of the divergent primers and cDNA from

cervical carcinoma HeLa cells yielded the detection of circEYA1. The convergent primers can only amplify the linear transcripts from no matter of whether cDNA or genomic DNA (gDNA). Glyceraldehyde 3-phosphate dehydrogenase (GAPDH) was shown as a linear transcript control (Figure 1E). The circular structure of circEYA1 was further confirmed by treatment of RNase R exonuclease, which degrades linear RNA but not circRNA. Figure 1F showed that circEYA1 were resistant to RNase R treatment, and RNase R treatment suppressed the linear transcripts of EYA1 amplified from HeLa cells. Taken together, these data demonstrated the existence of circEYA1 in cervical adenocarcinoma.

circEYA1 Inhibits Cell Viability and Colony-Formation Abilities and Promotes Apoptosis of Cervical Adenocarcinoma Cells

To study the biological function of circEYA1, circEYA1 was overexpressed in HeLa cells to test its effect on cell viability and cell apoptosis. Figure 2A showed circEYA1 expression levels in the overexpressing cells. Cell Counting Kit-8 (CCK-8) assays demonstrated that upregulation of circEYA1 significantly inhibited cell viability (Figure 2B). Similarly, the formed colonies of HeLa cells were markedly reduced by the presence of circEYA1 (Figure 2C). Annexin-V/propidium iodide (PI) staining with flow cytometry analysis showed that HeLa transfected with circEYA1 vector had a higher apoptotic rate than cells transfected with empty vector (Figure 2D).

To further explore the effects of circEYA1 on tumor growth *in vivo*, mouse xenograft models were established. circEYA1 overexpression significantly decreased tumor growth (Figure 2E). The tumors derived from cells overexpressing circEYA1 were much smaller (Figure 2E), which suggests circEYA1 significantly inhibits tumor growth. Consistent with this, immunohistochemistry (IHC) staining of the xenograft tumor tissues further demonstrated a decreased expression level of Ki-67 protein and an increased TUNEL-positive staining in circEYA1-overexpressing cells (Figure 2F). These results further confirmed the tumor-suppressive role of circEYA1 in cervical adenocarcinoma cells.

circEYA1 Acts as a Sponge for miR-582-3p

To elucidate the molecular mechanisms of circEYA1-suppressing cervical adenocarcinoma tumorigenesis, we first predicted the potential circEYA1/miRNA interaction using the Circular RNA Interactome database (<http://circinteractome.nia.nih.gov/index.html>). We have also conducted miRNA sequencing from the same cervical tissue samples and identified the differentially expressed miRNAs (DEmiRNAs) in cervical adenocarcinoma tissues. We have uploaded the descriptions of the miRNA sequencing data to GEO datasets (GEO: GSE145372). The putative miRNA candidates generated from the Interactome database were mapped to these DEmiRNA candidates, and we found that miR-582-3p was the only miRNA that was also significantly increased in cervical adenocarcinoma tissues. We first detected the expression of miR-582-3p in the same 20 cervical normal and adenocarcinoma tissues as well as HeLa cells by qRT-PCR. The results showed that miR-582-3p was markedly upregulated in cervical adenocarcinoma tissues and HeLa cells (Figure 3A). On the contrary,

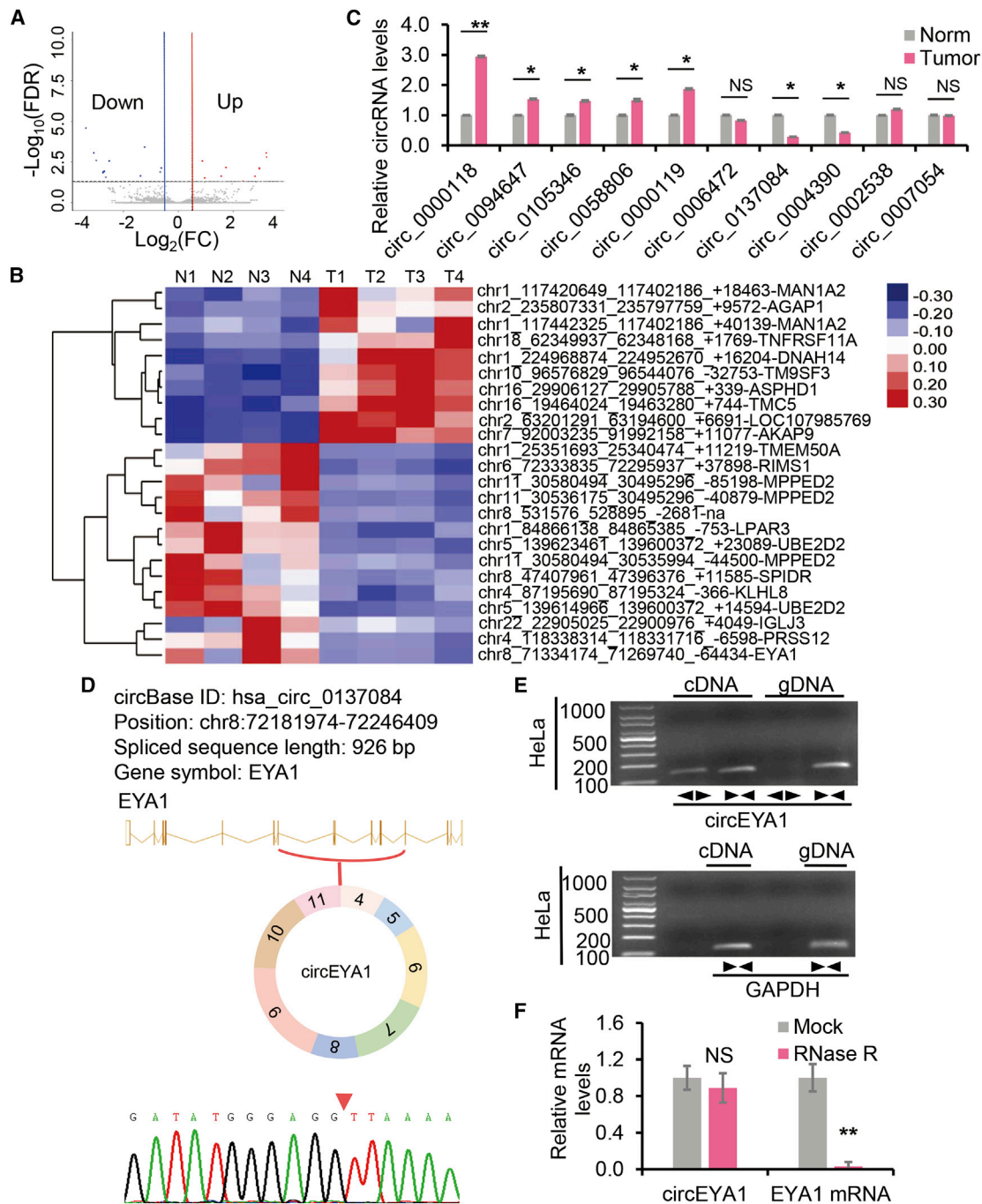


Figure 1. circRNA Expression Profile in Cervical Adenocarcinoma and Characterization of circEYA1

(A) Volcano plots illustrated the expression of circRNAs between 4 cervical adenocarcinoma tissues and 4 cervical normal tissues. The red dots and blue dots represent significantly statistically upregulated and downregulated circRNAs, respectively. (B) Heatmap of the 24 differentially expressed circRNAs in cervical adenocarcinoma tissues versus normal tissues. Red, upregulated circRNAs in cervical adenocarcinoma or normal tissues; blue, downregulated circRNAs in cervical adenocarcinoma or normal tissues. (C) Relative expression of circRNAs in cervical adenocarcinoma tissues (Tumor, $n = 20$) and 20 cervical normal tissues (Norm, $n = 20$) was detected by qRT-PCR. (D) circEYA1 is located at chromosome 8 and back-spliced by exons 4 and 11 of EYA1. The PCR products of circEYA1 were verified by Sanger sequencing. (E) The existence of circEYA1 was validated in cervical adenocarcinoma HeLa cells by RT-PCR. Divergent primers detected circEYA1 from cDNA, but not from genomic DNA (gDNA). GAPDH was used as a negative control for a linear RNA transcript. (F) qRT-PCR was used to determine the abundance of circEYA1 and linear EYA1 mRNA after treatment with RNase R in HeLa cells. circEYA1 was resistant to RNase R treatment. NS, not significant; * $p < 0.05$; ** $p < 0.01$.

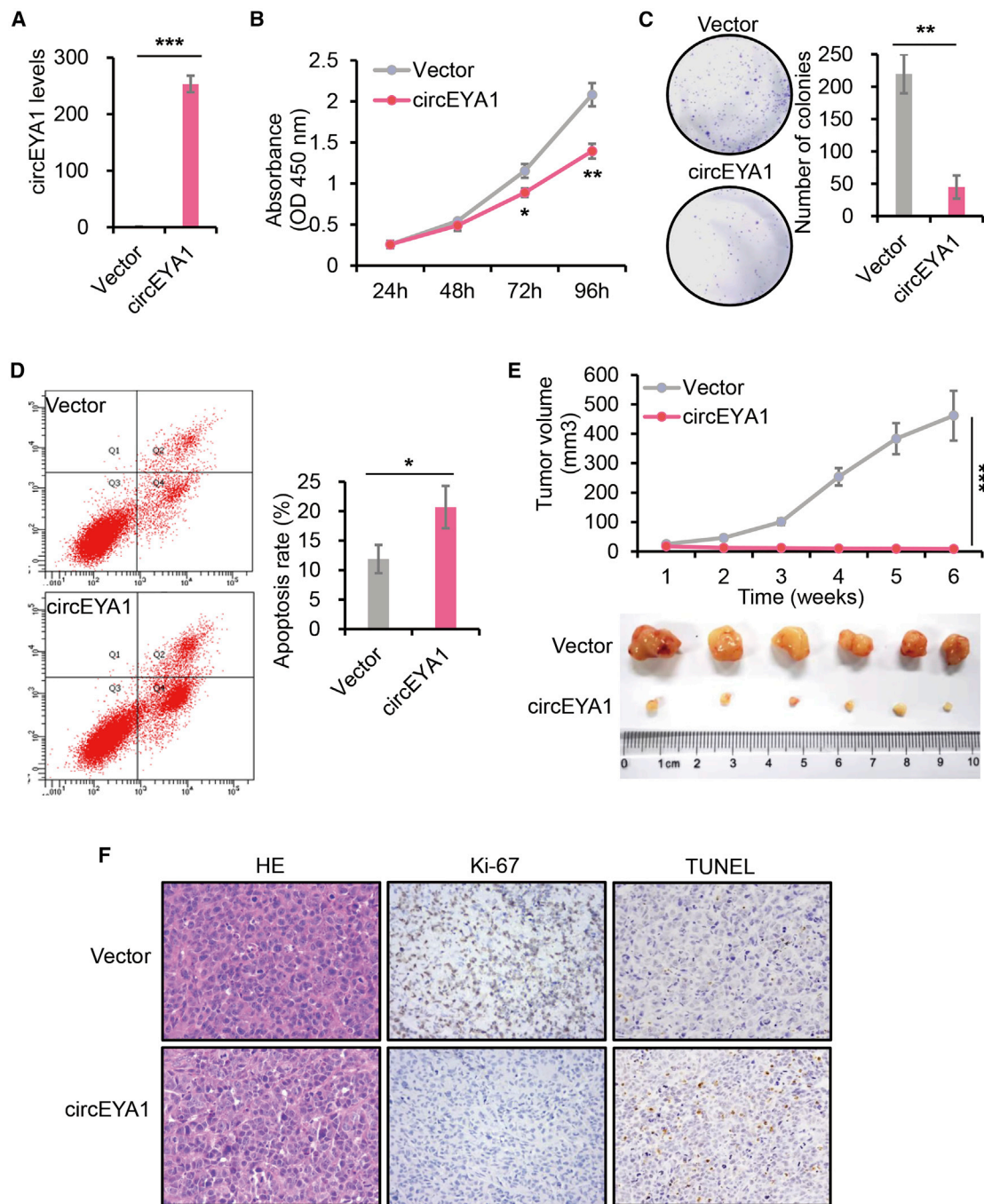


Figure 2. circEYA1 Produces Suppressive Effects on Cervical Adenocarcinoma Cells *In Vitro* and *In Vivo*

(A) qRT-PCR analysis of circEYA1 expression after transfection with circEYA1 expression vectors. (B and C) circEYA1 suppressed cell viability shown by CCK-8 (B) and colony formation (C) assays. (D) circEYA1 promoted cell by Annexin-V and PI assay. (E) HeLa cells with overexpression of circEYA1 or the vector control were inoculated in BALB/c nude mice (5×10^6 cells per mouse, $n = 6$ for each group) to establish subcutaneous xenograft tumors. The growth curves and representative images of xenograft tumors are shown. The tumor volumes were measured once a week. (F) IHC staining revealed that the circEYA1 overexpression led to decreased Ki-67 expression and increase TUNEL-positive staining in the tumors. * $p < 0.05$; ** $p < 0.01$; *** $p < 0.001$.

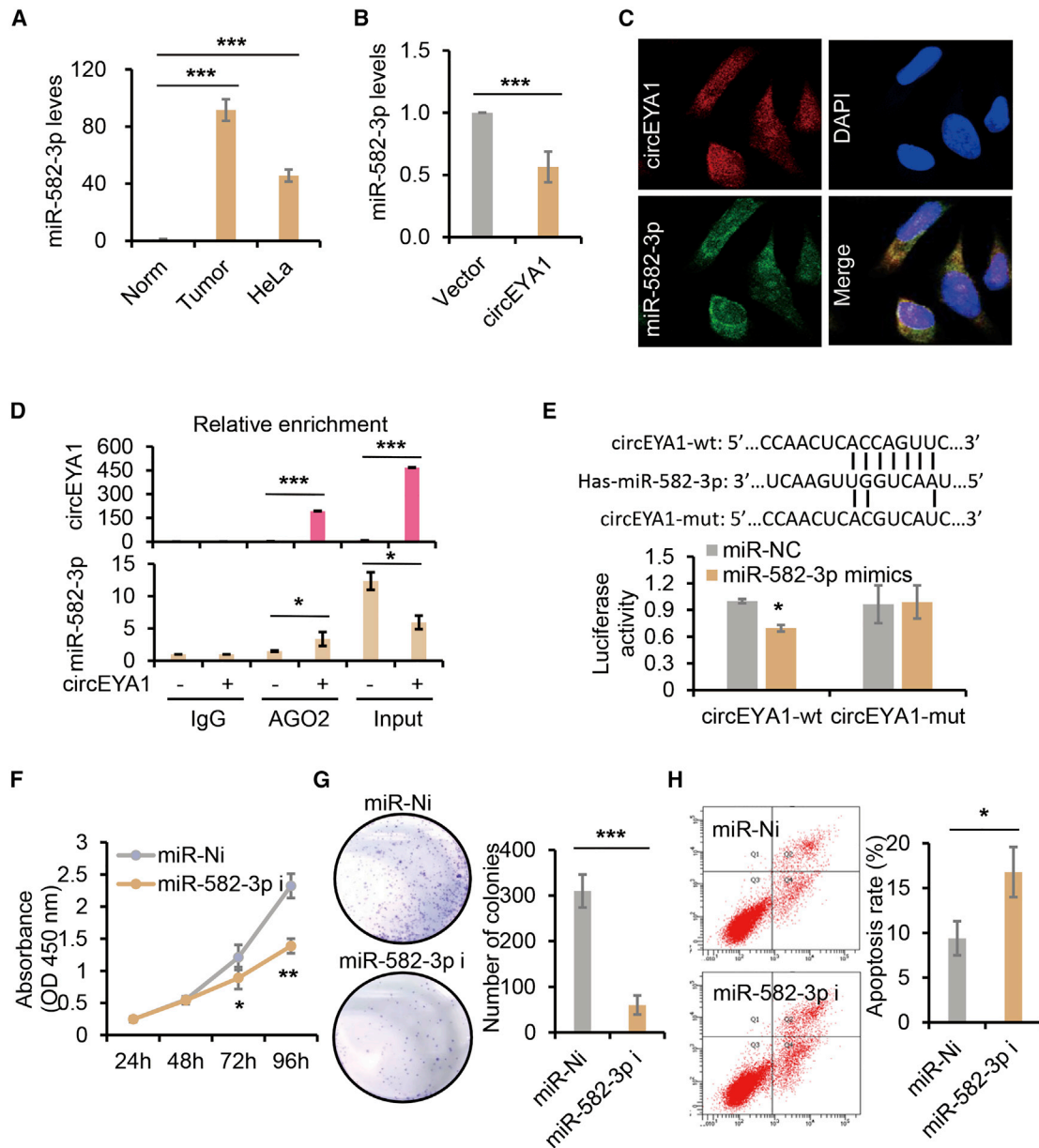


Figure 3. circEYA1 Serves as a Sponge of miR-582-3p

(A) The relative expression of miR-582-3p in cervical adenocarcinoma tissues (Tumor, n = 20), normal tissues (Norm, n = 20), and HeLa cells was examined by qRT-PCR. (B) Relative expression of miR-582-3p was evaluated in HeLa cells after transfection with circEYA1 or empty vector. (C) The cellular location of circEYA1 (red) and miR-582-3p (green) in HeLa cells was detected by FISH. (D) Anti-AGO2 RIP was executed in HeLa cells after transfection with circEYA1 or empty vector, and qRT-PCR was detected for the enrichment of circEYA1 and miR-582-3p. (E) The schematic of circEYA1-wt and circEYA1-mut luciferase reporter vector is shown. The relative luciferase activities were determined in 293T cells co-transfected with miR-582-3p mimics or miR-NC and the wild-type or mutant luciferase reporter, respectively. (F and G) Cell viability was detected after transfection with miR-582-3p inhibitors (miR-582-3p i) or miR-Ni by CCK-8 and colony-formation assay, respectively. (H) Cell apoptosis was determined by Annexin-V and PI assay after transfection. *p < 0.05; **p < 0.01; ***p < 0.001.

overexpression of circEYA1 significantly decreased miR-582-3p expression levels in HeLa cells (Figure 3B). To check whether circEYA1 and miR-582-3p are colocalized, the fluorescence *in situ* hybridization (FISH) assay was applied to HeLa cells, and we observed

that most of circEYA1 and miR-582-3p were co-located in both the cytoplasm and the nucleus (Figure 3C). This observation does not exclude the possibility that circEYA1 and miR-582-3p keep close proximity through a third player. The Argonaute protein AGO2 is

known as a binding substrate of miRNAs, and here we tested this opportunity by performing an anti-AGO2 RNA immunoprecipitation (RIP) assay in HeLa cells overexpressing circEYA1. The results showed that both miR-582-3p and circEYA1 could bind to AGO2 and also revealed that miR-582-3p was predominantly enriched in the circEYA1-overexpressed group compared with the control (Figure 3D). In addition, to test the interaction between circEYA1 and miR-582-3p, a dual-luciferase reporter assay showed that miR-582-3p mimics could significantly decrease the luciferase activity of the circEYA1-wild-type (wt) group but not the circEYA1-mut group (Figure 3E), suggesting a direct interaction between circEYA1 and miR-582-3p. Since circEYA1 counteracts miR-582-3p activities, it is naive to propose that miR-582-3p has opposite effects in cervical adenocarcinoma compared with circEYA1. To test this, we applied miR-582-3p inhibitors to HeLa cells and confirmed that inhibition of miR-582-3p markedly reduced cell viability (Figure 3F) and colony formation (Figure 3G) and promoted cell apoptosis (Figure 3H).

To further validate that circEYA1 functions as a miR-582-3p sponge, a series of rescue experiments were performed using the same approaches as mentioned above. The CCK-8 and colony-formation assays showed that circEYA1-dependent inhibition of cell growth was reversed by miR-582-3p overexpression in HeLa cells (Figures 4A and 4B). miR-582-3p could also reverse the apoptosis-promoting effects induced by circEYA1 overexpression (Figure 4C). In addition, experiments using the xenograft mouse model showed that decreased tumor growth after overexpression of circEYA1 was at least partially reversed by treatment with miR-582-3p mimics (Figure 4D). In summary, all these data demonstrated that circEYA1 functions through sponging miR-582-3p in cervical adenocarcinoma.

CXCL14 Is Identified as a Direct Target of miR-582-3p

To verify how circEYA1 sponges miR-582-3p and liberates the expression of its downstream targets, we identified the potential target genes of miR-582-3p by using the TargetScan prediction program. According to the ceRNA (competing endogenous RNA) theory, we also filtered genes that were positively associated with circEYA1 in our RNA sequencing data. As a result, 24 candidate target genes were found (Figure 5A). 7 of these potential target genes were further determined. Moreover, miR-582-3p inhibitors could strongly increase calneuron 1 (CALN1) and C-X-C motif chemokine ligand 14 (CXCL14) expression, while miR-582-3p mimics markedly suppressed CALN1 and CXCL14 expression (Figure 5B). Also, the protein levels of CALN1 and CXCL14 were accordingly decreased after miR-582-3p mimics (Figure 5C). To further determine the protein levels of the CXCL14 secreted extracellularly, we conducted an enzyme-linked immunosorbent assay (ELISA, 4A Biotech, China) using the culture supernatant from HeLa cells with or without miR-582-3p overexpression or inhibition. HeLa cells treated with miR-582-3p inhibitors secreted more CXCL14 protein, while the CXCL14 level was significantly decreased in HeLa cells transfected with miR-582-3p mimics (Figure S3). To verify whether CALN1 and CXCL14 were the direct targets of miR-582-3p, we performed dual-luciferase reporter assay. We found that the activity of luciferase reporter vector

carrying the CALN1 3'-UTR-wt or CXCL14 3'-UTR-wt sequence could be significantly impaired by miR-582-3p mimics compared with each negative control group (Figures 5D and S4A). The luciferase activity was not changed when co-transfected with CALN1 3'-UTR mutant or CXCL14 3'-UTR mutant vector (Figures 5D and S4A). However, the anti-proliferative effects induced by miR-582-3p inhibitors could not be significantly reversed by specific si-CALN1#1 or si-CALN1#2 in HeLa cells (Figure S4B), indicating that CALN1 might not participate in miR-582-3p-dependent cell growth, though it is a target protein regulated by miR-582-3p.

Thus, we focused on CXCL14 for its roles in circEYA1/miR-582-3p signaling. The expression levels of CXCL14 were first validated by qRT-PCR and western blot analysis in HeLa cells transfected with the p-CXCL14 expression vector in HeLa cells by qRT-PCR and western blot analysis (Figure S5). Cell viability and colony formation ability were significantly suppressed by ectopic expression of CXCL14 in HeLa cells (Figures 5E and 5F). In addition, the anti-proliferative effects caused by miR-582-3p inhibitors was counteracted by inhibition of CXCL14 using specific si-CXCL14#1 or si-CXCL14#2 in HeLa cells (Figure 5G). Also, knockdown of CXCL14 could abrogate the effects of miR-582-3p inhibitors on promoting cell apoptosis (Figures 5H and S6A). These data indicate that CXCL14 is the direct functional target gene of miR-582-3p.

circEYA1 Increases CXCL14 Expression by Partly Sponging miR-582-3p

To confirm that circEYA1 can act as a ceRNA to regulate CXCL14 expression, we measured the expression levels of CXCL14 in HeLa cells with circEYA1 overexpression. The results showed that ectopic expression of circEYA1 significantly increased CXCL14 mRNA and protein levels (Figures 6A and 6B). The RIP assay on AGO2 showed that circEYA1, miR-582-3p, and CXCL14 were mainly enriched to AGO2 (Figures 3E and 6C). Moreover, the increased expression of CXCL14 mRNA and protein induced by circEYA1 overexpression could be partially reversed by miR-582-3p mimics (Figures 6D and 6E). In addition, specific si-CXCL14#1 and si-CXCL14#2 could rescue circEYA1-mediated suppression for cell viability and colony formation ability of HeLa cells, respectively (Figures 6F and 6G). Moreover, knockdown of CXCL14 could partially rescue the pro-apoptotic effects of HeLa cells with ectopic expression of circEYA1 (Figures 6H and S6B). These results revealed that circEYA1 sponges miR-582-3p to regulate the expression of CXCL14 and suppresses cell viability via a ceRNA mechanism in HeLa cells.

The Correlation and Diagnostic Value of the circEYA1/miR-582-3p/ CXCL14 Axis in Clinical Human Cervical Tissue Samples

To confirm the association among circEYA1, miR-582-3p, and CXCL14 in clinical cervical tissues, the expression of these molecules was verified in another independent cohort of 198 human cervical tissue samples, including 57 normal and 141 adenocarcinoma tissues, by qRT-PCR. As expected, circEYA1 was markedly downregulated in cervical adenocarcinoma tissues compared with the normal group, whereas miR-582-3p was strongly upregulated (Figure 7A). We also

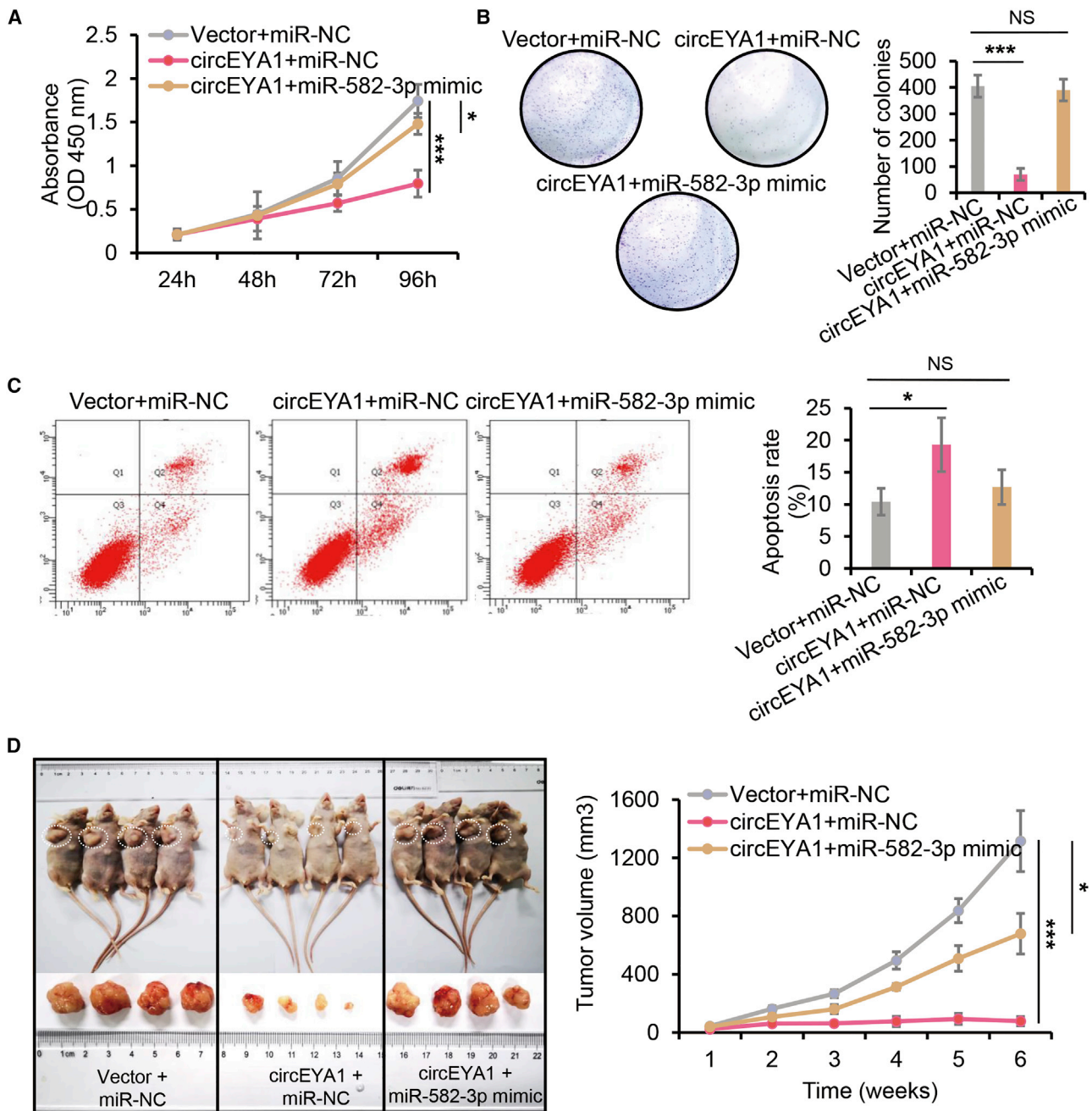
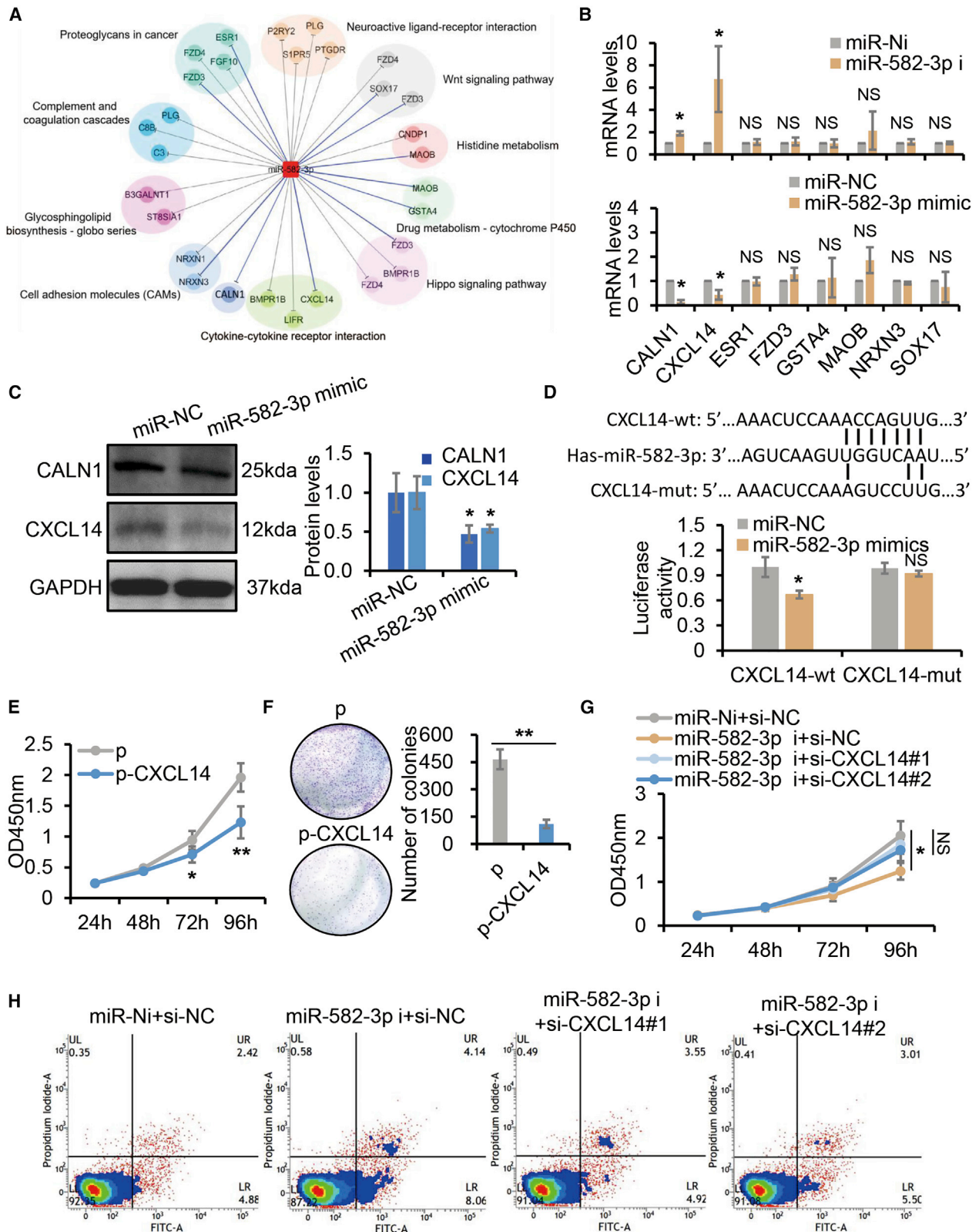


Figure 4. circEYA1 Exerts Tumor-Suppressive Effects through Sponging miR-582-3p

(A and B) miR-582-3p mimics partially reversed the effects of circEYA1 on cell viability by CCK-8 assay (A) and colony-formation assay (B), respectively. (C) miR-582-3p mimics partially abolished the effects of circEYA1 on cell apoptosis by Annexin-V and PI assay. (D) Xenograft models were established. The growth curves and representative images of xenograft tumors showed that miR-582-3p overexpression reversed the tumor-suppressive roles of circEYA1 on tumor growth. NS, not significant; * $p < 0.05$; *** $p < 0.001$.

found CXCL14 significantly downregulated in cervical adenocarcinoma tissues (Figure 7A). Then, we verified whether any correlation existed among these candidates, Pearson's correlation analysis exhibited a significantly inverse correlation between circEYA1 and

miR-582-3p, a positive correlation between circEYA1 and CXCL14, and negative correlation between miR-582-3p and CXCL14 (Figure 7B). Therefore, we suppose that the circEYA1/miR-582-3p/CXCL14 axis exists in cervical adenocarcinoma tissue samples.



(legend on next page)

To explore the diagnostic potential of these molecules, we conducted receiver operating characteristic (ROC) curve analysis. As shown in Figure 7C, the area under the curve (AUC) to discriminate cervical adenocarcinoma from normal tissues was 0.814 (95% confidence interval [CI], 0.754–0.874) for circEYA1, 0.919 (95% CI, 0.882–0.956) for miR-582-3p, and 0.729 (95% CI, 0.654–0.805) for CXCL14 (Figure 7C). Our results suggest the high diagnostic potential of these three candidates in patients with cervical adenocarcinoma.

DISCUSSION

Recent next-generation sequencing approaches have led to the discovery of numerous circRNAs in multiple cell lines and tissues.²² Due to stable molecular structure and cell/tissue-specific expression pattern, circRNAs could function as oncogenic stimuli or tumor suppressors in many types of cancers, such as gastric cancer, hepatocellular carcinoma, breast cancer, and bladder cancer.^{18,23–25} However, only a few circRNAs have been functionally well-explored. The expression profile of circRNAs as well as their biological function remain unknown in cervical adenocarcinoma.

In our study, we applied RNA sequencing to detect differentially expressed circRNAs within 4 cervical adenocarcinoma tissues relative to 4 cervical normal tissues. We subsequently verified 11 circRNAs in another 40 clinical cervical tissue samples and identified hsa_circ_0137084, termed circEYA1, as the most obviously downregulated circRNA in cervical adenocarcinoma. We have demonstrated that circEYA1 overexpression significantly suppressed cell viability and promoted apoptosis of cervical adenocarcinoma cells. We also confirmed that circEYA1 overexpression inhibited tumorigenesis in xenograft mouse models. Our findings indicate that circEYA1 acts as a tumor suppressor in the development of cervical adenocarcinoma, and it might be a novel diagnostic marker or therapy target for cervical adenocarcinoma patients.

Although the mechanisms of how circRNA acts as a regulator in cancers have not been fully explored, growing evidence has shown that circRNAs can function as ceRNAs to regulate the expression of miRNA targets in tumor biology.^{25–27} For example, circRNA cRAP-GEF5 functions as a sponge of miR-27a-3p and abates its repression on the target gene TXNIP to suppress proliferation and migration of renal cell carcinoma cells.²⁸ It was reported that circNFIX acted as a ceRNA of miR-378e to relieve the suppressive effect of miR-378e on its target gene RPN2 and promoted progression of glioma.²⁹ Here,

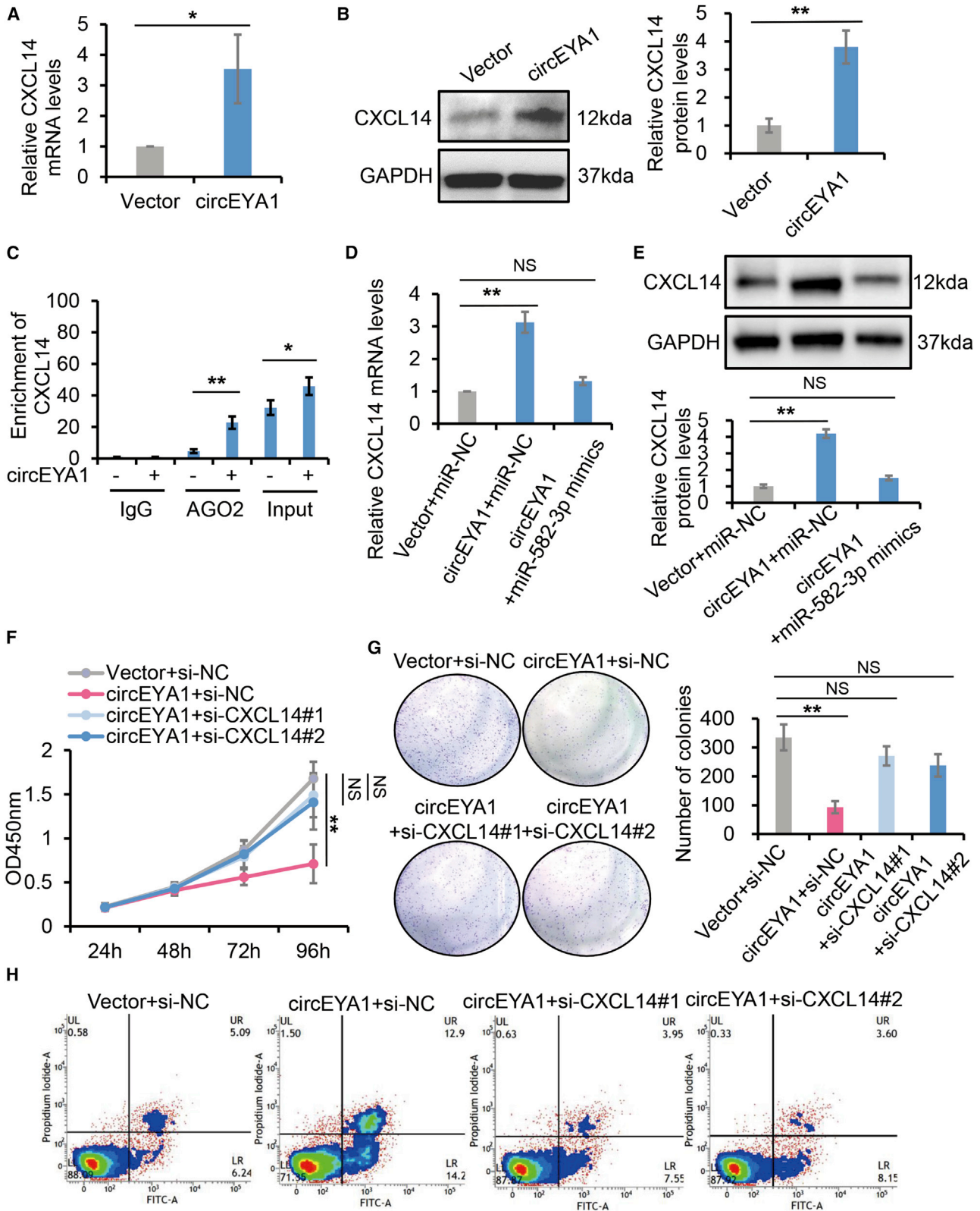
our studies provided more evidence to support this idea. Of note, the binding efficiency between circEYA1 and miR-582-3p from FISH assay and RIP analysis might be different. For AGO2-RIP, the transfection with circEYA1 vector may impact the binding rate of circEYA1 on AGO2 in the treated HeLa cells, whereas in the FISH assay we detected the basal expression level of circEYA1 and miR-582-3p in HeLa cells. The different expression levels of circEYA1 might determine the difference in these two experiments. In addition, the observation from the FISH assay could not exclude the possibility that circEYA1 and miR-582-3p keep close proximity through a third player. Further studies are needed to address this question. As the binding miRNA of circEYA1, miR-582-3p inhibition phenocopied the biological effects of circEYA1 overexpression in cervical adenocarcinoma cells. Consistently, overexpression of miR-582-3p reversed the suppressive behaviors of circEYA1 *in vitro* and *in vivo*. Our results suggest that circEYA1 serves as a tumor suppressor by sponging miR-582-3p in cervical adenocarcinoma cells.

In addition to revealing the novel role of circEYA1 in cervical adenocarcinoma, our studies pointed out the critical role of miR-582-3p in the same disease. Our data clearly showed that miR-582-3p was significantly increased in cervical adenocarcinoma compared with normal cervical tissues and that miR-582-3p exerts tumor oncogenic roles and targets multiple genes associated with cancer-related pathways. Similarly, the aberrant expression of miR-582-3p was found in several tumors, such as colon cancer,³⁰ non-small cell lung carcinoma (NSCLC),³¹ and non-functioning pituitary adenomas.⁴ For instance, miR-582-3p expression was markedly upregulated in NSCLC and positively correlated with the recurrence-free and overall survival of NSCLC patients.³¹ On the other hand, miR-582-3p was also found decreased in Hodgkin's lymphoma³² and bladder cancer.³³ These studies indicate that miR-582-3p acts as oncogenic or tumor-suppressive miRNA in a tumor-type-dependent manner.

According to the ceRNA hypothesis, circEYA1 may act as a ceRNA to regulate the expression of miR-582-3p target genes. We first reported CXCL14 as a direct functional target gene of miR-582-3p and indirect target of circEYA1. CXCL14 belongs to the CXC subfamily of cytokines. It was reported that CXCL14 was significantly downregulated in hepatitis B virus-related hepatocellular carcinoma tissues. Cicchini et al.³⁴ also reported that CXCL14 was dramatically downregulated in HPV-positive head/neck and cervical cancers and suppressed by the HPV oncogene E7. They further revealed that restoration of CXCL14

Figure 5. CXCL14 Is a Direct Functional Target Gene of miR-582-3p

(A) Expression relation of miR-582-3p-target mRNA network. Putative miR-582-3p target genes were predicted by TargetScan and analyzed by KEGG pathway. The genes involved in the main pathways were shown. (B) qRT-PCR validated the relative expression levels of selected putative targets including CALN1, CXCL14, ESR1, FZD3, GSTA4, MAOB, NRXN3, and SOX17 in HeLa cells after transfection with miR-582-3p i or miR-582-3p mimics or indicated negative controls. (C) The relative expression of CALN1 and CXCL14 protein was assessed in cells transfected with miR-582-3p mimics by western blot. (D) The schematic of CXCL14-wt and CXCL14-mut luciferase reporter vectors were shown. The relative luciferase activities were analyzed in 293T cells co-transfected with miR-582-3p mimics or miR-NC and the CXCL14-wt or CXCL14-mut luciferase reporter vectors. (E) CCK-8 assay of cell viability after transfection with CXCL14 expression plasmid or empty plasmid in HeLa cells. (F) Colony-formation assay was determined after transfection with CXCL14 expression plasmid or empty plasmid in HeLa cells. (G) Cell viability assay was detected by CCK-8 assay after transfected miR-582-3p inhibitors or co-transfected miR-582-3p inhibitors and specific si-CXCL14#1 or si-CXCL14#2. (H) Cell apoptosis assay for HeLa cells with miR-582-3p inhibition and joint knockdown of CXCL14 was determined by Annexin-V and PI assay after transfection. NS, not significant; *p < 0.05; **p < 0.01.



(legend on next page)

expression in HPV-positive oropharyngeal carcinoma cells could clear tumors in immunocompetent syngeneic mice. Here, we found that CXCL14 was significantly downregulated in cervical adenocarcinoma tissues, and overexpression of CXCL14 could inhibit cell viability in HeLa cells. Its expression can be regulated by circEYA1 via sponging miR-582-3p's activities.

To sponge miR-582-3p, circEYA1 has to locate together with and act as a ceRNA to regulate the expression of miR-582-3p target genes. Our studies by RIP assay validated the interaction among circEYA1, miR-582-3p, and CXCL14 (Figures 3E and 6C), which is consistent with the observation of Figure 3B. CXCL14 has been shown to be suppressed by HPV oncogene E7;³⁴ thus, we determined whether HPV18 E7 regulates CXCL14 through the alteration of expression of circEYA1 and miR-582-3p in cervical adenocarcinoma cells. Surprisingly, the expression levels of circEYA1 and miR-582-3p were not significantly changed upon HPV18 E7 knockdown, indicating that CXCL14 expression is regulated in an HPV E7-independent manner (Figure S7). Finally, correlation analysis showed that circEYA1, miR-582-3p, and CXCL14 were tightly correlated. To better represent our conclusions, Figure 7D schematically illustrates a mechanism cartoon showing that circEYA1 functions as a ceRNA of miR-582-3p to relieve the repressive effect of miR-582-3p on its target gene, CXCL14. In addition, ROC analysis revealed that circEYA1, miR-582-3p, and CXCL14 held good potential applicable value as diagnostic markers for cervical adenocarcinoma.

The main limitation of our studies is the cell resource. The current available cervical adenocarcinoma cell lines are only HeLa and HeLa-derived cells, such as HeLa 229, GH345, and HeLa S3. Other cervical cancer cell lines, including SiHa, CaSki, C33A, C4I-1/2, MS751, and ME180, are all CSCC cells. To ensure the validity of observation from the cell line, we had to validate our results in a large cohort of cervical adenocarcinoma tissues and animal models. As cervical adenocarcinoma attracts more attention, we believe new cervical adenocarcinoma cell lines will be developed for research purposes in the near future.

In conclusion, our study revealed the expression profile of circRNAs and identified circEYA1 as the most significantly downregulated circRNA in human cervical adenocarcinoma tissues. We demonstrated that circEYA1 functions as a sponge of miR-582-3p to abolish the suppressive effect of miR-582-3p on CXCL14 and then inhibits cell viability. We suggest that circEYA1 could be a promising therapeutic target and diagnostic marker for cervical adenocarcinoma in the future.

MATERIALS AND METHODS

Human Patient Samples and Ethical Approval

All human cervical adenocarcinoma and squamous cell carcinoma tissues and normal cervical tissues were obtained from patients who had undergone surgery at the Women's Hospital, Zhejiang University School of Medicine (Hangzhou, China). Cervical tumor tissues were obtained from patients with primary cervical tumors who underwent radical hysterectomy with pelvic lymph node dissection. Normal cervical tissues without HPV infection were obtained from women who underwent hysterectomy for nonmalignant diseases. This study was approved by the Ethics Committee of the Women's Hospital of Zhejiang University (IRB-2019062-R) and conducted in accordance with the Declaration of Helsinki. Written informed consent was obtained from all patients. All tissue samples were placed immediately in liquid nitrogen after removal from the patients and stored at -80°C until use.

RNA Sequencing

RNA sequencing was performed by NovelBio Laboratory, Shanghai, China. The RNA sequencing data have been uploaded to GEO datasets (GSE: 145372). Generally, RNA extracted by Trizol reagent (Invitrogen) was utilized to construct rRNA depletion library (NEBNext Ultra Directional RNA Library Prep Kit) according to the manufacturer's instructions. RNA sequencing data sequenced by HiSeq Sequencer was filtered and mapped to the human genome (Bta genome version 5.0.1 NCBI) utilizing HISAT2.³⁵ circRNA was predicted based on the sequencing data with the ACFS2 circRNA prediction pipeline.³⁶ Differentially expressed gene analysis was applied utilizing DESeq³⁷ under the following criteria: fold change > 2 , or fold change < 0.5 ; FDR < 0.05 .

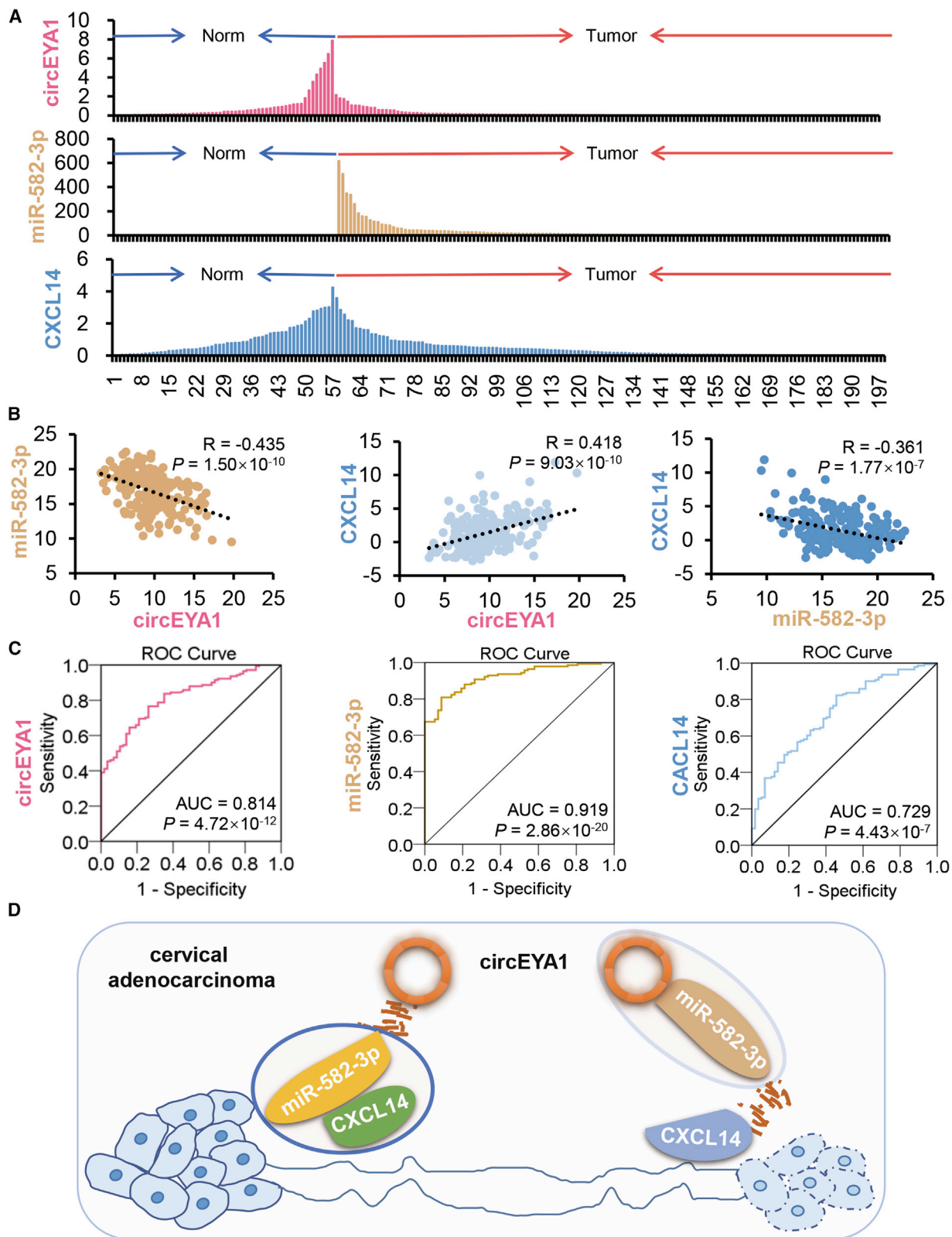
RNA Extraction, Treatment with RNase R, gDNA Extraction, and qRT-PCR Analysis

All RNAs were extracted from tissues and cells by using Trizol reagent (Invitrogen). For RNase R treatment, 2 mg total RNA was incubated for 15 min at 37°C with or without RNase R (Epicenter Technologies). cDNA synthesis was performed using the PrimeScript RT reagent kit with gDNA Eraser (TaKaRa). gDNA was isolated from cultured cells by using the PureLink Genomic DNA Mini Kit (Thermo Fisher Scientific).

Samples were performed on a StepOne Plus Real-Time PCR System (Applied Biosystems) using TB Green Premix Ex Taq kit (TaKaRa). We used GAPDH and U6 as internal controls. Relative RNA levels were analyzed using the $2^{-\Delta\Delta\text{Ct}}$ method. miRNA primers were bought from Biomics Biotech, Nantong, China. The primer sequences are listed in Table S2.

Figure 6. circEYA1 Increases CXCL14 Expression by Partly Sponging miR-582-3p

(A and B) The relative expression of CXCL14 mRNA and protein was evaluated in cells after transfection with circEYA1 by qRT-PCR (A) and western blot (B), respectively. (C) As part of the Figure 3E results, RIP assay showed the enrichment of CXCL14 and circEYA1 on AGO2. (D and E) circEYA1 increased the expression of CXCL14 mRNA (D) and protein (E) in HeLa cells; this effect could be partially reversed by co-transfection with miR-582-3p mimics (D and E). (F) Cell viability assay for HeLa cells with circEYA1 overexpression and joint knockdown of CXCL14 siRNA #1 or #2. (G) Colony-formation analysis for HeLa cells with circEYA1 overexpression and CXCL14 knockdown. (H) Cell apoptosis assay for HeLa cells with circEYA1 overexpression and CXCL14 knockdown. NS, not significant; * $p < 0.05$; ** $p < 0.01$.



(legend on next page)

Cell Culture and Transfection

Cervical adenocarcinoma HeLa cells were purchased from the Shanghai Institute of Biochemistry and Cell Biology, Chinese Academy of Sciences (Shanghai, China). The cells were cultured in MEM medium (Cellmax). All culture media contained 10% fetal bovine serum (FBS) (Sijiqing, China), 100 U/mL penicillin, and 100 U/mL streptomycin (Invitrogen). The cells were determined to be mycoplasma-free and incubated at 37°C with 5% CO₂.

A human circEYA1 expression vector, pLC5-ciR-circEYA1, and a control vector, pLC5-ciR, were bought from GENESEED, China. The human CXCL14 expression plasmid pcDNA3.1+/CXCL14 and empty plasmid pcDNA3.1+ were bought from TSINGKE, China. miR-582-3p mimics, miR-582-3p inhibitors, CALN1 siRNAs, CXCL14 siRNAs, HPV18 E7 siRNAs, and negative controls were all purchased from GenePharma, China. Plasmids were transfected into cervical adenocarcinoma cells using X-tremeGENE HP DNA transfection reagent (Roche, USA). The miRNA mimics and miRNA inhibitors were transfected using DharmaFECT1 transfection reagent (Dharmacon) as per manufacturer's protocol. Co-transfection of plasmids and miRNA mimics were performed using Lipofectamine 3000 (Invitrogen).

FISH

Cy3-labeled circEYA1 and FITC-labeled miR-582-3p probes were designed and synthesized by GENESEED, China. Probe sequences were for hsa_circEYA1-CY3: 5'-GCTCTGTTTAAACCTCCCATATCT-3' and for hsa-miR-582-3p-FITC: 5'-TTCAGTTGTCAACCAGTTA-3'. The probe signals were determined by a FISH kit (Ribobio, China) according to the manufacturer's instructions. The HeLa cells were treated with 4',6-diamidino-2-phenylindole (DAPI) (Life Technologies) as the control. Confocal images were acquired on a laser confocal microscope (TCS SP2 AOBS). Each experiment was repeated three times independently.

RIP

The EZ-Magna RIP Kit (Millipore) was used according to the manufacturer's instructions. HeLa cells were lysed in RIP lysis buffer, and the cell extract was then incubated with magnetic beads conjugated with anti-Argonaute 2 (AGO2) or control anti-IgG antibody (Abcam). The beads were washed and incubated with Proteinase K, and the purified RNA was finally subjected to qRT-PCR analysis. Each experiment was repeated three times independently.

Luciferase Reporter Assays

Potential binding sites of miR-582-3p on circEYA1, CALN1, and CXCL14 were predicted by Circular RNA Interactome and

TargetScan database. The different fragment sequences were synthesized, inserted into the pmiRGLO vector (Promega), and then verified by sequencing. Luciferase activities were measured by the Dual-Luciferase Reporter Assay Kit (Promega) according to the manufacturer's protocols. Each assay was performed in triplicate and repeated three times independently.

CCK-8 Assays

HeLa cells were seeded into 96-well plates at 3,000 cells/well and transfected with indicated circRNA expression vectors, miRNA inhibitors, or miRNA mimics. CCK-8 solution (Dojindo) was added to each well and incubated for 1 h at 24, 48, 72, and 96 h post-transfection. The optical density (OD) values were determined on a spectrophotometer reader (Thermo Fisher) at 450 nm. Each assay was performed in triplicate and repeated three times independently.

Colony-Formation Assays

Colony-formation assays were performed to monitor cervical adenocarcinoma cell cloning capability. Treated HeLa cells (5,000 cells/well) were seeded into 6-well plates and incubated for 10 days for colony-formation assays. The colonies were fixed in 70% ethanol for 10 min and stained with 2% crystal violet solution for 5 min at room temperature. Images were acquired with a camera (Canon). All assays were performed three independent times.

Cell Apoptosis Assays

Treated cells were resuspended in binding buffer containing annexin V-fluorescein isothiocyanate (FITC) and PI for 15 min in the dark (MultiSciences, China). The apoptosis rate was measured with a FACSCalibur or FACSVerse flow cytometer (BD Biosciences). The experiments were repeated three times independently.

Western Blotting

Treated cells were lysed and equivalent amounts of total protein were separated by 10% SDS-PAGE gel and transferred onto polyvinylidene fluoride (PVDF) membranes (Merck). The membranes were incubated with primary antibodies, followed by a secondary antibody. Anti-CALN1 and anti-CXCL14 were purchased from Proteintech and Abcam, respectively. Anti-GAPDH antibody (Santa Cruz) was used as an internal control. Proteins were detected by using a SuperSignal West Pico Chemiluminescent Substrate (Pierce) and Quantity One software. All experiments were repeated three times independently.

Mouse Xenograft Model

The animal experiments were performed in accordance with the Institute for Laboratory Animal Research Guide for the Care and

Figure 7. Characterization of circEYA1, miR-582-3p, and CXCL14 in Clinical Cervical Adenocarcinoma Tissues

(A) Distribution of expression levels of circEYA1, miR-582-3p, and CXCL14 in 57 normal cervical and 141 cervical adenocarcinoma tissue samples by qRT-PCR. Data of these expression levels are shown as fold change levels of adenocarcinoma versus average normal controls. (B) Pearson's correlation analysis showed that circEYA1 negatively correlated with miR-582-3p, whereas it positively correlated with CXCL14 in these 198 clinical cervical tissue samples. miR-582-3p negatively correlated with CXCL14. (C) Receiver operating characteristic (ROC) curve analysis of circEYA1, miR-582-3p, and CXCL14 detection for cervical adenocarcinoma diagnosis. (D) Proposed function and mechanism of circEYA1 in cervical adenocarcinoma.

Use of Laboratory Animals and approved by the Institutional Animal Care and Use Committee (IACUC) of Zhejiang Chinese Medical University (approval no. IACUC-20190909-02). Female BALB/c nude mice, age 4 weeks, were purchased from the Shanghai National Laboratory Animal Center and then housed and cared for under standard recommended conditions in the animal research center of Zhejiang Chinese Medical University. HeLa cells with overexpressed circEYA1 or control vector or co-transfected with miR-582-3p mimics or miR-NC were harvested. For the tumor growth assay, 5×10^6 cells were subcutaneously injected into the right single flank of each mouse. Tumor growth was measured every week, and tumor volume was calculated with the following formula: $\text{volume (mm}^3\text{)} = (\text{length} \times \text{width}^2) / 2$. Six weeks after injection, the mice were euthanized by the cervical dislocation method. The tumors were removed and fixed for H&E and Ki-67 staining and TUNEL assay.

Statistical Analysis

Data analyses were carried out with GraphPad Prism 6.0 (GraphPad Software) and SPSS 24.0 (SPSS). Data are expressed as the mean \pm SD and calculated difference by either Student's t test or Mann-Whitney U test. Statistical significance was defined as $p < 0.05$. * $p < 0.05$, ** $p < 0.01$, *** $p < 0.001$, and NS stands for not significant.

SUPPLEMENTAL INFORMATION

Supplemental Information can be found online at <https://doi.org/10.1016/j.omtn.2020.10.026>.

ACKNOWLEDGMENTS

Our work was supported by the National Key Research and Development Program of China 2016YFC1302900 (W.L.), the National Natural Science Foundation of China 81702552 and 82072855 (J.X.), and Fundamental Research Funds for the Central Universities of China 2019QNA7035 (J.X.).

AUTHOR CONTRIBUTIONS

J.X. and W.L. conceived the project and designed the study. J.X., Y.Z., and Y.H. developed methodology. J.X., Y.Z., Y.H., X.D., Z.X., J.Z., and L.W. performed experiments. J.X., Y.Z., Y.H., and X.D. analyzed the data. J.X., Y.Z., and Y.H. wrote the manuscript. W.L. revised the manuscript. The study supervisor is W.L. All authors read and approved the final manuscript.

DECLARATION OF INTERESTS

The authors declare no competing interests.

REFERENCES

- Bray, F., Ferlay, J., Soerjomataram, I., Siegel, R.L., Torre, L.A., and Jemal, A. (2018). Global cancer statistics 2018: GLOBOCAN estimates of incidence and mortality worldwide for 36 cancers in 185 countries. *CA Cancer J. Clin.* *68*, 394–424.
- Smith, H.O., Tiffany, M.F., Qualls, C.R., and Key, C.R. (2000). The rising incidence of adenocarcinoma relative to squamous cell carcinoma of the uterine cervix in the United States—a 24-year population-based study. *Gynecol. Oncol.* *78*, 97–105.
- Sasieni, P., and Adams, J. (2001). Changing rates of adenocarcinoma and adenocarcinoma of the cervix in England. *Lancet* *357*, 1490–1493.
- Visioli, C.B., Zappa, M., Ciatto, S., Iossa, A., and Crocetti, E. (2004). Increasing trends of cervical adenocarcinoma incidence in Central Italy despite Extensive Screening Programme, 1985–2000. *Cancer Detect. Prev.* *28*, 461–464.
- Bray, F., Carstensen, B., Møller, H., Zappa, M., Zakelj, M.P., Lawrence, G., Hakama, M., and Weiderpass, E. (2005). Incidence trends of adenocarcinoma of the cervix in 13 European countries. *Cancer Epidemiol. Biomarkers Prev.* *14*, 2191–2199.
- Castellsagué, X., Díaz, M., de Sanjosé, S., Muñoz, N., Herrero, R., Franceschi, S., Peeling, R.W., Ashley, R., Smith, J.S., Snijders, P.J., et al.; International Agency for Research on Cancer Multicenter Cervical Cancer Study Group (2006). Worldwide human papillomavirus etiology of cervical adenocarcinoma and its cofactors: implications for screening and prevention. *J. Natl. Cancer Inst.* *98*, 303–315.
- Adegoke, O., Kulasingam, S., and Virnig, B. (2012). Cervical cancer trends in the United States: a 35-year population-based analysis. *J. Womens Health (Larchmt.)* *21*, 1031–1037.
- Oh, C.M., Jung, K.W., Won, Y.J., Shin, A., Kong, H.J., Jun, J.K., and Park, S.Y. (2013). Trends in the incidence of in situ and invasive cervical cancer by age group and histological type in Korea from 1993 to 2009. *PLoS ONE* *8*, e72012.
- Bulk, S., Visser, O., Rozendaal, L., Verheijen, R.H., and Meijer, C.J. (2005). Cervical cancer in the Netherlands 1989–1998: Decrease of squamous cell carcinoma in older women, increase of adenocarcinoma in younger women. *Int. J. Cancer* *113*, 1005–1009.
- Gien, L.T., Beauchemin, M.C., and Thomas, G. (2010). Adenocarcinoma: a unique cervical cancer. *Gynecol. Oncol.* *116*, 140–146.
- van der Horst, J., Siebers, A.G., Bulten, J., Massuger, L.F., and de Kok, I.M. (2017). Increasing incidence of invasive and in situ cervical adenocarcinoma in the Netherlands during 2004–2013. *Cancer Med.* *6*, 416–423.
- Guarnerio, J., Bezzi, M., Jeong, J.C., Paffenholz, S.V., Berry, K., Naldini, M.M., Lo-Coco, F., Tay, Y., Beck, A.H., and Pandolfi, P.P. (2016). Oncogenic Role of Fusion-circRNAs Derived from Cancer-Associated Chromosomal Translocations. *Cell* *166*, 1055–1056.
- Du, W.W., Yang, W., Liu, E., Yang, Z., Dhaliwal, P., and Yang, B.B. (2016). Foxo3 circular RNA retards cell cycle progression via forming ternary complexes with p21 and CDK2. *Nucleic Acids Res.* *44*, 2846–2858.
- Xiong, D.D., Dang, Y.W., Lin, P., Wen, D.Y., He, R.Q., Luo, D.Z., Feng, Z.B., and Chen, G. (2018). A circRNA-miRNA-mRNA network identification for exploring underlying pathogenesis and therapy strategy of hepatocellular carcinoma. *J. Transl. Med.* *16*, 220.
- Qu, S., Zhong, Y., Shang, R., Zhang, X., Song, W., Kjems, J., and Li, H. (2017). The emerging landscape of circular RNA in life processes. *RNA Biol.* *14*, 992–999.
- Yang, Y., Fan, X., Mao, M., Song, X., Wu, P., Zhang, Y., Jin, Y., Yang, Y., Chen, L.L., Wang, Y., et al. (2017). Extensive translation of circular RNAs driven by N⁶-methyladenosine. *Cell Res.* *27*, 626–641.
- Hansen, T.B., Jensen, T.I., Clausen, B.H., Bramsen, J.B., Finsen, B., Damgaard, C.K., and Kjems, J. (2013). Natural RNA circles function as efficient microRNA sponges. *Nature* *495*, 384–388.
- Yang, R., Xing, L., Zheng, X., Sun, Y., Wang, X., and Chen, J. (2019). The circRNA circAGFG1 acts as a sponge of miR-195-5p to promote triple-negative breast cancer progression through regulating CCNE1 expression. *Mol. Cancer* *18*, 4.
- Wu, L., Li, Y., Xu, X.M., and Zhu, X. (2019). Circular RNA circ-PRKCI promotes cell proliferation and invasion by binding to microRNA-545 in gastric cancer. *Eur. Rev. Med. Pharmacol. Sci.* *23*, 9418–9426.
- Wang, L., Liang, Y., Mao, Q., Xia, W., Chen, B., Shen, H., Xu, L., Jiang, F., and Dong, G. (2019). Circular RNA circCRIM1 inhibits invasion and metastasis in lung adenocarcinoma through the microRNA (miR)-182/miR-93-leukemia inhibitory factor receptor pathway. *Cancer Sci.* *110*, 2960–2972.
- Zhang, X., Wang, S., Wang, H., Cao, J., Huang, X., Chen, Z., Xu, P., Sun, G., Xu, J., Lv, J., and Xu, Z. (2019). Circular RNA circNRIP1 acts as a microRNA-149-5p sponge to promote gastric cancer progression via the AKT1/mTOR pathway. *Mol. Cancer* *18*, 20.
- Sheng, J.Q., Liu, L., Wang, M.R., and Li, P.Y. (2018). Circular RNAs in digestive system cancer: potential biomarkers and therapeutic targets. *Am. J. Cancer Res.* *8*, 1142–1156.

23. Xiong, D.D., Feng, Z.B., Lai, Z.F., Qin, Y., Liu, L.M., Fu, H.X., He, R.Q., Wu, H.Y., Dang, Y.W., Chen, G., and Luo, D.Z. (2019). High throughput circRNA sequencing analysis reveals novel insights into the mechanism of nitidine chloride against hepatocellular carcinoma. *Cell Death Dis.* *10*, 658.
24. Shen, F., Liu, P., Xu, Z., Li, N., Yi, Z., Tie, X., Zhang, Y., and Gao, L. (2019). CircRNA_001569 promotes cell proliferation through absorbing miR-145 in gastric cancer. *J. Biochem.* *165*, 27–36.
25. Liu, L., Wu, S.Q., Zhu, X., Xu, R., Ai, K., Zhang, L., and Zhao, X.K. (2019). Analysis of ceRNA network identifies prognostic circRNA biomarkers in bladder cancer. *Neoplasma* *66*, 736–745.
26. Salmena, L., Poliseno, L., Tay, Y., Kats, L., and Pandolfi, P.P. (2011). A ceRNA hypothesis: the Rosetta Stone of a hidden RNA language? *Cell* *146*, 353–358.
27. Ma, X., Liu, C., Gao, C., Li, J., Zhuang, J., Liu, L., Li, H., Wang, X., Zhang, X., Dong, S., et al. (2020). circRNA-associated ceRNA network construction reveals the circRNAs involved in the progression and prognosis of breast cancer. *J. Cell. Physiol.* *235*, 3973–3983.
28. Chen, Q., Liu, T., Bao, Y., Zhao, T., Wang, J., Wang, H., Wang, A., Gan, X., Wu, Z., and Wang, L. (2020). CircRNA cRAPGEF5 inhibits the growth and metastasis of renal cell carcinoma via the miR-27a-3p/TXNIP pathway. *Cancer Lett.* *469*, 68–77.
29. Ding, C., Wu, Z., You, H., Ge, H., Zheng, S., Lin, Y., Wu, X., Lin, Z., and Kang, D. (2019). CircNFIX promotes progression of glioma through regulating miR-378e/RPN2 axis. *Journal of experimental & clinical cancer research. J. Exp. Clin. Cancer Res.* *38*, 506.
30. Bobowicz, M., Skrzypski, M., Czapiewski, P., Marczyk, M., Maciejewska, A., Jankowski, M., Szulgo-Paczkowska, A., Zegarski, W., Pawlowski, R., Polańska, J., et al. (2016). Prognostic value of 5-microRNA based signature in T2-T3N0 colon cancer. *Clin. Exp. Metastasis* *33*, 765–773.
31. Fang, L., Cai, J., Chen, B., Wu, S., Li, R., Xu, X., Yang, Y., Guan, H., Zhu, X., Zhang, L., et al. (2015). Aberrantly expressed miR-582-3p maintains lung cancer stem cell-like traits by activating Wnt/ β -catenin signalling. *Nat. Commun.* *6*, 8640.
32. Paydas, S., Acikalin, A., Ergin, M., Celik, H., Yavuz, B., and Tanriverdi, K. (2016). Micro-RNA (miRNA) profile in Hodgkin lymphoma: association between clinical and pathological variables. *Med. Oncol.* *33*, 34.
33. Uchino, K., Takeshita, F., Takahashi, R.U., Kosaka, N., Fujiwara, K., Naruoka, H., Sonoke, S., Yano, J., Sasaki, H., Nozawa, S., et al. (2013). Therapeutic effects of microRNA-582-5p and -3p on the inhibition of bladder cancer progression. *Mol. Ther.* *21*, 610–619.
34. Cicchini, L., Westrich, J.A., Xu, T., Vermeer, D.W., Berger, J.N., Clambey, E.T., Lee, D., Song, J.I., Lambert, P.F., Greer, R.O., et al. (2016). Suppression of Antitumor Immune Responses by Human Papillomavirus through Epigenetic Downregulation of CXCL14. *MBio* *7*, e00270-16.
35. Kim, D., Langmead, B., and Salzberg, S.L. (2015). HISAT: a fast spliced aligner with low memory requirements. *Nat. Methods* *12*, 357–360.
36. You, X., Vlatkovic, I., Babic, A., Will, T., Epstein, I., Tushev, G., Akbalik, G., Wang, M., Glock, C., Quedenau, C., et al. (2015). Neural circular RNAs are derived from synaptic genes and regulated by development and plasticity. *Nat. Neurosci.* *18*, 603–610.
37. Anders, S., and Huber, W. (2010). Differential expression analysis for sequence count data. *Genome Biol.* *11*, R106.